Simultaneously Enhancing Aggregation-Induced Emission and Boosting Two-Photon Absorption of Perylene Diimides through Regioisomerization

Liang Xu,* Xueting Long, Fangyuan Kang, Ziqi Deng, Jiaxin He, Sirui Yang, Jieyu Wu, Lingfeng Yin, Xiao-Fang Jiang, Fushen Lu, Ming-De Li, and Qichun Zhang*

L. Xu, X. Long, J. He, S. Yang, L. Yin, F. Lu, M. Li, Department of Chemistry and Key Laboratory for Preparation and Application of Ordered Structural Materials of Guangdong Province, Shantou University, Guangdong 515063, China, E-mail: xuliang@stu.edu.cn

F. Kang, Q. Zhang, Department of Materials Science and Engineering, City University of Hong Kong, Kowloon, Hong Kong SAR, China, E-mail: qiczhang@cityu.edu.hk

Z. Deng, Department of Chemistry, University of Hong Kong, Hong Kong, China

J. Wu, Prof. X. Jiang, Laboratory of Quantum Engineering and Quantum Material, School of Physics and Telecommunication Engineering, South China Normal University, Guangzhou 510006, China

Q. Zhang, Center of Super-Diamond and Advanced Films (COSDAF), City University of Hong Kong, Hong Kong SAR, 999077, P. R. China

Table of contents

1. Experimental Section

1.1 Equipment and measurement conditions

Synthesis and characterization of the AIE molecules. All the AIE molecules were synthesized using Suzuki-coupling protocols as detailed in Supplementary Information. Chemical structures were confirmed by ^{1}H NMR and ^{13}C NMR spectroscopy using a Brucker-Biosipin Avance 400 MHz spectrometer in $CDCl_3$ at room temperature.

Optical property spectroscopy. UV-Vis absorption spectra and fluorescence emission spectra were determined with a Shimadzu UV-Vis-2600 spectrophotometer and a Shimadzu RF-6000 spectrophotometer.

Transient absorption spectroscopy. The fs-TA measurements were performed based on a femtosecond Ti:sapphire regenerative amplified Ti: sapphire laser system (Coherent, Astrella) and an automated data acquisition system (Ultra-fast Systems, HeliosFire). The half pulse width of output from amplifier is 80 fs. The probe pulse was obtained by using approximately 1 W of the amplified 800 nm output from the Spitfire to generate a white-light continuum (320-780 nm) in a sapphire plate or CaF_2 crystal. The maximum extent of the temporal delay was 8000 ps. The instrument response function was determined to be 200 fs. At each temporal delay, data were averaged for 2 s and collected by the acquisition system. The probe beam was split into two before passing through the sample. One probe beam traveled through the sample, the other was sent directly to the reference spectrometer that monitored the fluctuations in the probe beam intensity. Fiber optics was coupled to a multichannel spectrometer with a CMOS sensor that had a 1.5 nm intrinsic resolution. For the experiments described in this study, the sample solution was excited by a 525 nm pump beam which is obtained by using femtosecond TOPAS amplifier. The solutions were excited in a 2 mm path-length cuvette with a sample concentration of 0.2 mM throughout the data acquisition. The data were stored as three-dimensional (3D) wavelength-time-absorbance matrices that were exported for use with the fitting software. Therefore, in order to remove the contributions of the solvent, the raw spectra of the sample were subtracted by the spectra of the solvent under the same

conditions.

Kinetics fitting method. Equation 1 shows the exponential function for wavelength kinetics fitting. The wavelength kinetics fitting for **B-PDI-ANT** and **O-PDI-ANT** are both fitted by three exponential functions and result in three lifetimes at 430 nm.

$$S(t) = e^{-(\frac{t-t_0}{t_p})^2} * \sum_i A_i e^{-\frac{t-t_0}{t_i}}, \quad t_p = \frac{IRF}{2\ln 2} \qquad \text{Equation 1}$$

Potential energy surface scanning method. The potential surface energy scanning (PES) was obtained from DFT and TD-DFT calculation using Gaussian 16, employing M062X method and 6-311g (d,p) basis set. The scanning mainly investigates the energy change with different dihedral between perylene ring and the anthracene ring. The step size was set to be 10 degree from -10°to -170° (The situation in 0°was excluded because the two rings were totally overlapped). The energy of the optimized geometry at ground state was set as 0, and all energy in PES used the relative energy.

Two-photon excited fluorescence spectroscopy. A homemade spectrofluorometer was used while a femtosecond pulsed laser (Chameleon Discovery NX, Coherent), with pulse duration, ≈140 fs (FWHM), 80 MHz, repetition rate, tuning range 800-1100 nm served as the excitation source. 2PA measurements were performed in 10 mm spectrofluorometric quartz cuvettes with the dye concentrations of 5×10^{-5} M. Possible reabsorption of fluorescence emission was analyzed and taken into account. The quadratic dependence of two-photon induced fluorescence intensity on the excitation power was checked for each excitation wavelength. The reference is Rhodamine B with a concentration of 5×10^{-5} M solution in spectroscopic grade methanol. The samples are measured in spectroscopic grade THF. In the measuring range of excitation wavelengths, from 800 to 1100 nm, linear absorption could be neglected for all of the solutions. For comparison, the 2PA spectrum of PDI parent is also measured at the same condition.

Open-aperture Z-scan measurement. The sample concentrations are 1×10^{-2} M for B-PDI-ANT and 6×10^{-3} M for O-PDI-ANT. The wavelength is set to be 1100nm. The 2PA cross-section is determined by translating the sample around the focal plane of a Gaussian beam, while obtaining the transmittance change in the far field. The power transmitted

through a nonlinear absorptive material, for a spatially and temporally a Gaussian beam, can be integrated. The normalized beam transmittance is expressed by

$$T(z) = \frac{1}{\sqrt{\pi} q_0(z,0)} \int_{-\infty}^{\infty} \ln\left[1 + q_0(z,0) e^{-\tau^2}\right] d\tau \quad Equation\ 2$$

$$q_0 = \beta I_0 L_{eff} \left(1 + \left(\frac{z^2}{z_0^2}\right)\right)^{-1} \quad Equation\ 3$$

Where, z is the distance between the sample and the focus; z_0 is the Rayleigh diffraction length; I_0 is the peak power density; $L_{eff} = (1 - e^{-\alpha_0 L})/\alpha_0$ is the effective length and L is the sample length; β is the nonlinear absorption coefficient. The 2PA absorption coefficient β is obtained by fitting the experimental transmittance data with Eq. 2. The 2PA cross section is thus calculated using the equation of $\delta = h\omega\beta/(2\pi N_0)$, where $h\omega/2\pi$ is the excitation photon energy and N_0 is the number of molecules per cm^3. 2PA cross section values are generally presented in GM (Göpert-Meyer) units, where 1 GM = 1×10^{-50} cm^4s/photon.

1.2 Synthesis of B-PDI-ANT

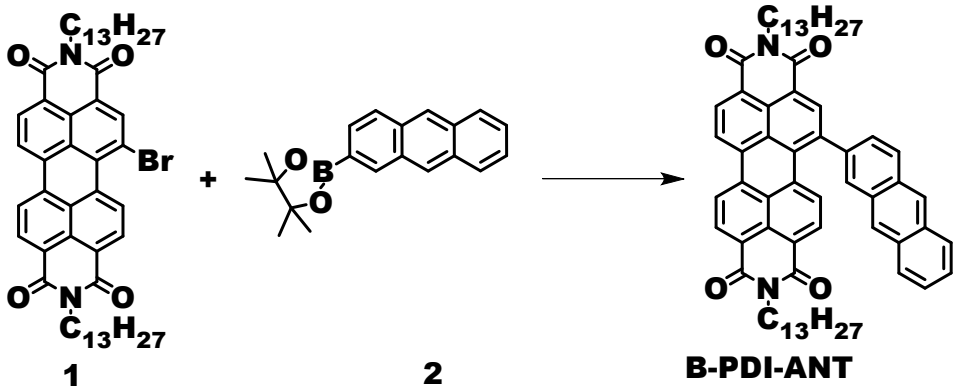

Scheme S1. The synthetic route to B-PDI-ANT.

Compounds **1** and **2** were synthesized according to the literature.[1-3] A mixture of **1** (0.4 g, 0.48 mmol),**2** (0.176 g, 0.58mmol), $Pd(PPh_3)_4$ (0.055 g, 0.047mmol), K_2CO_3(0.132g,0.96mmol),DMF (10 mL) was stirred at 80 °C under N_2 atmosphere for 24h. After coolingto room temperature, the solvent was removed under reduced pressure.Then the collected solid was redissolved in dichloromethane (100 mL) and washed with brine (100 mL) twice. The organic layer was dried

over $NaSO_4$ and concentrated by the rotary evaporator in vacuum. The crude product was further purified by column chromatography(DCM/petroleum ether=16:1 to 6:1) to give the desired product as the dark purple solid (372 mg, 0.4mmol, 83% yield).^{1}H NMR (400 MHz, $CDCl_3$) δ 8.79-8.61(m,5H), 8.51-8.46(d,2H), 8.36(s,1H), 8.06-7.99(m,4H), 7.96-7.93(d,1H), 7.55-7.51(m, 2H), 7.27-7.25 (d, 1H), 5.26-5.10(m,2H), 2.32-2.14(m,4H), 1.88-1.79(m,4H), 1.32-1.19(m,32H), 0.84-0.78(m,12H).^{13}C NMR (100 MHz, $CDCl_3$) δ 141.84, 140.01, 135.22, 135.00, 134.83, 132.88, 132.71, 131.21, 130.78, 130.66, 129.54, 129.03, 128.73, 128.58, 128.42, 127.89, 127.47, 127.04, 126.52, 126.39, 123.96, 123.13, 55.25, 55.12, 53.87, 32.86, 32.79, 32.23, 32.19, 31.89, 29.69, 27.38, 23.05, 14.50.

1.3 Synthesis of O-PDI-ANT

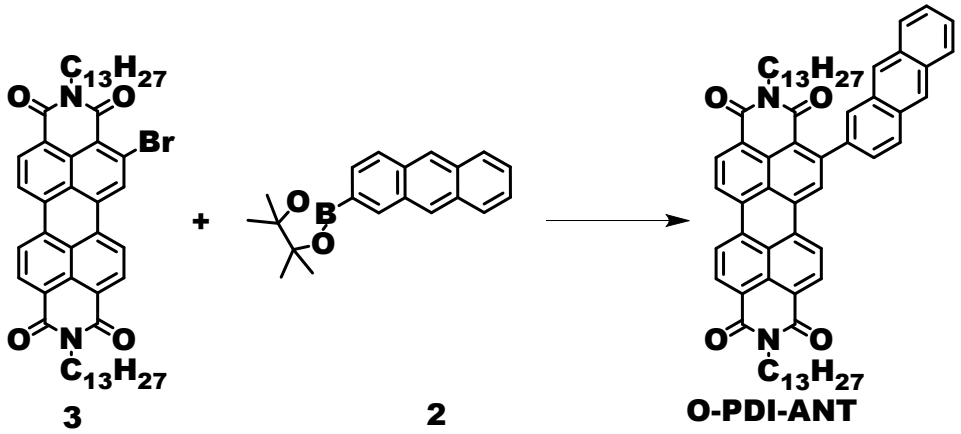

Scheme S2. The synthetic route to O-PDI-ANT.

Compounds **2** and **3** were synthesized according to the literature.[3-5]A mixture of **3** (0.2 g, 0.24 mmol), **2** (0.15 g, 0.48 mmol), $Pd(PPh_3)_4$ (0.03 g, 0.025 mmol), K_2CO_3(0.066g,0.48mmol),DMF (30 mL) was stirred at 80 °C under N_2 atmosphere for 24h. After cooling, remove DMF with rotary evaporator.Then the collected solid was redissolved in dichloromethane (100 mL) and washed with brine (100 mL) twice. The organic layer was dried over $NaSO_4$ and concentrated by the rotary evaporator in vacuum. The residue was then purified by silica gel column chromatography (petroleum ether/DCM=6:1 to 1:1). A dark red solid of O-PDI-AN (0.07g, 0.08mmol) was obtained in 33% yield.^{1}H NMR (400 MHz, $CDCl_3$) δ 8.74-8.54(m,7H), 8.38-8.33(d,2H), 8.06(s,1H), 7.97-7.91(d,3H), 7.43(s,3H), 5.20-5.02(m,2H), 2.29-2.21(m,4H), 1.90-1.79(m,4H), 1.34-

1.24(m,32H),0.88-0.81(m,12H).^{13}C NMR (100 MHz, $CDCl_3$) δ 134.55, 134.26, 131.98, 131.92, 131.52, 130.85, 130.77, 130.52, 128.58, 128.11, 128.01, 127.53, 126.92, 126.62, 126.39, 126.20, 125.53, 123.27, 123.02, 122.78, 54.75, 53.40, 32.39, 32.22, 31.76, 31.43, 30.19, 29.22, 26.94, 22.61, 14.07.

2. Characterization Section

2.1 ^{1}H and ^{13}C NMR

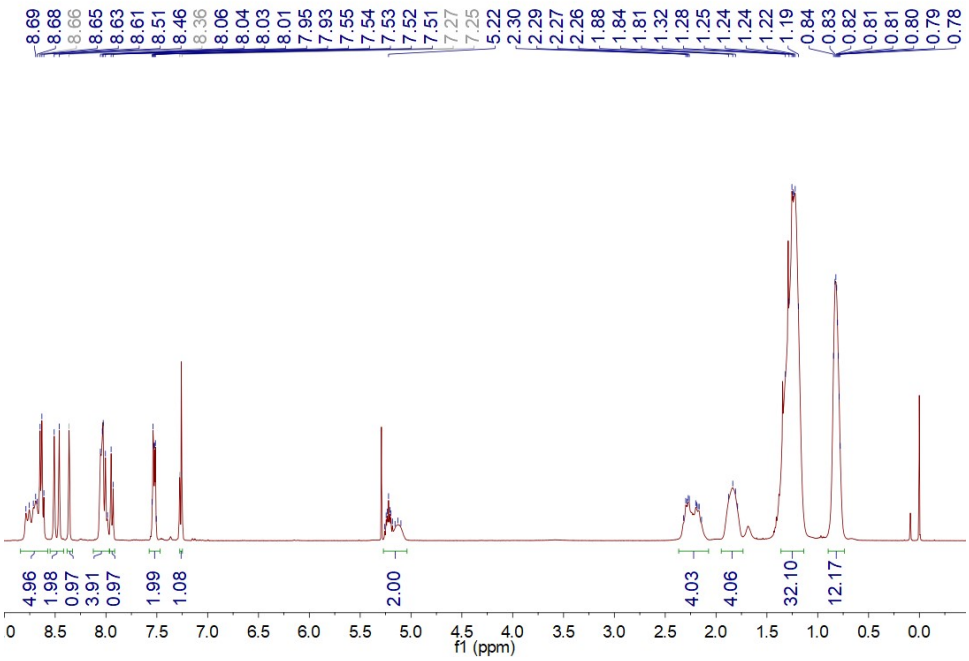

Figure S1.^{1}H NMR of B-PDI-ANT in chloroform-d.

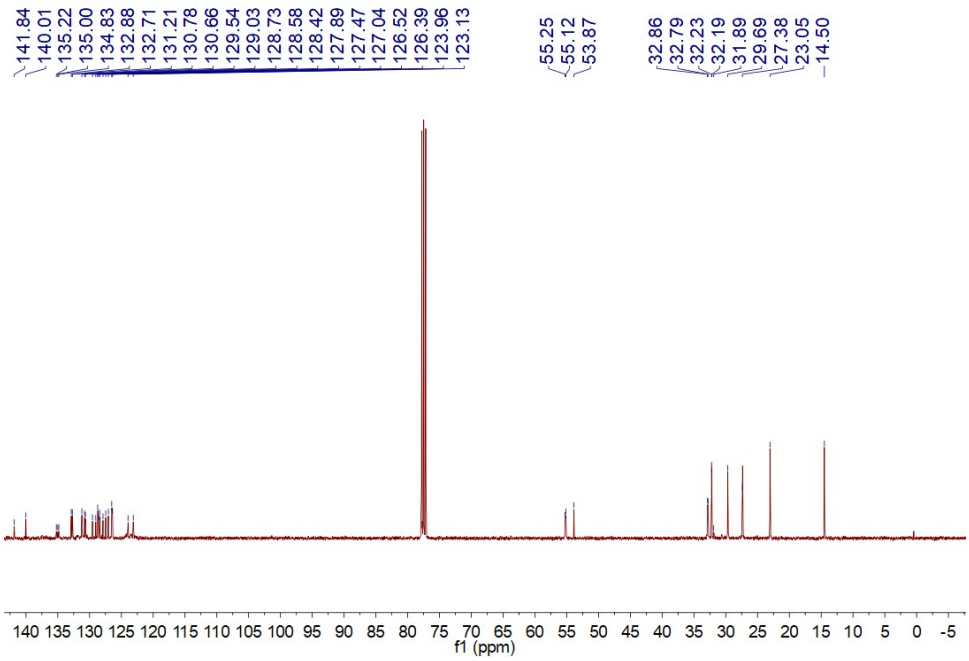

Figure S2.[13]C NMR of B-PDI-ANT in chloroform-d.

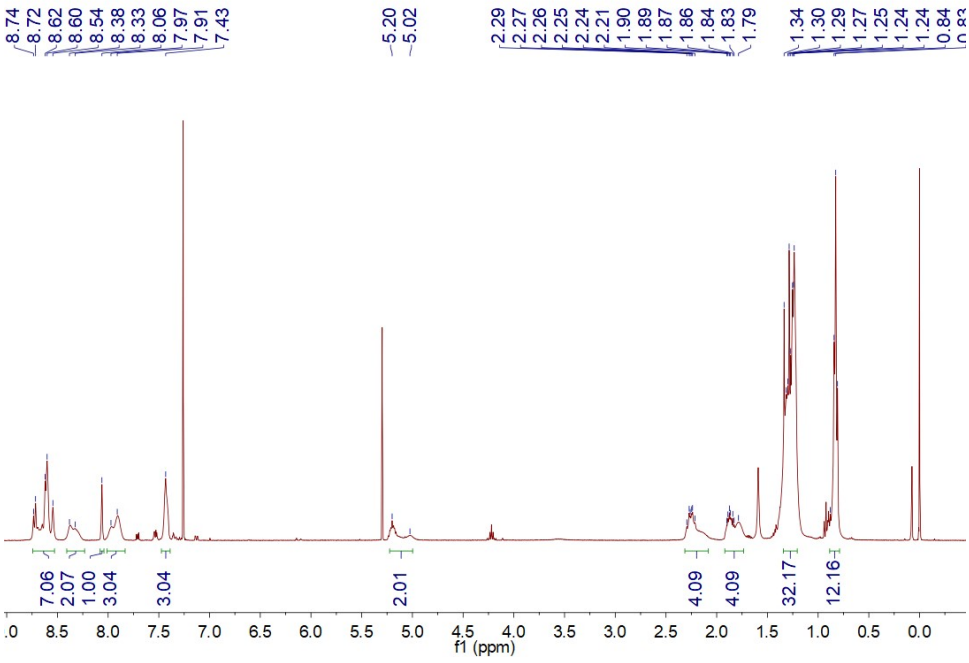

Figure S3.[1]H NMR of O-PDI-ANT in chloroform-d.

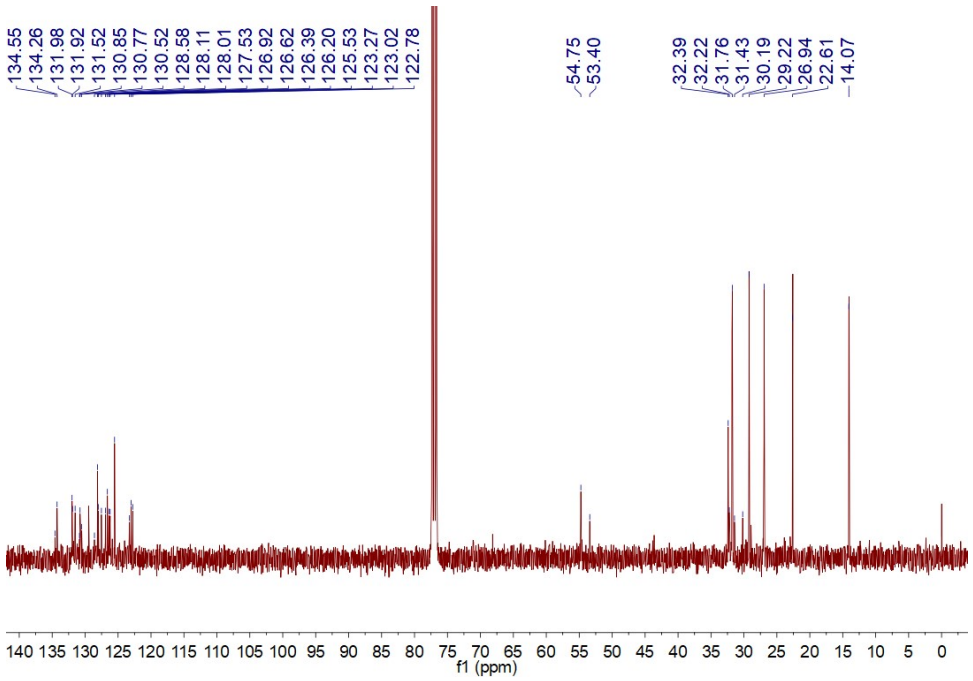

Figure S4.^{13}C NMR of O-PDI-ANT in chloroform-d.

2.2 The fluorescence emission spectra of B-PDI-ANT and O-PDI-ANT in various of solvents with different viscosities

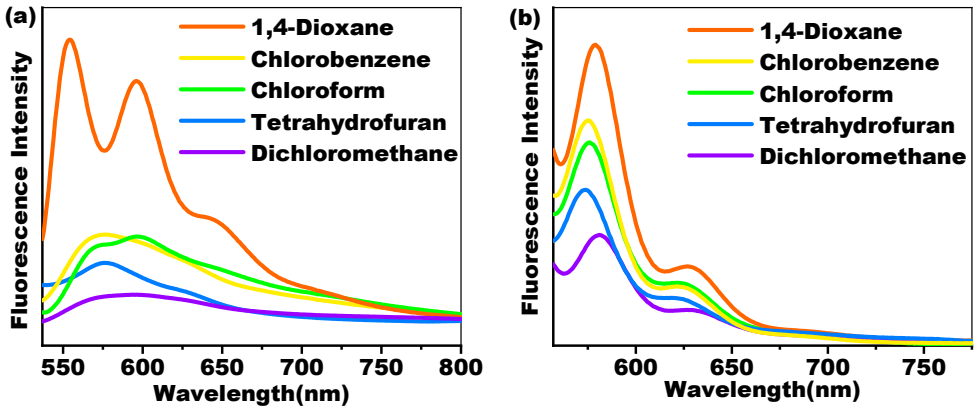

Figure S5. The fluorescence emission behaviors of (a) B-PDI-ANT and (b) O-PDI-ANT in five good solvents with different viscosities. The excitation wavelength of fluorescence emission spectra for B-PDI-ANT and O-PDI-ANT is 525 nm

2.3 The dynamic light scattering (DLS) study on nanoparticle size distribution of B-PDI-ANT and O-PDI-ANT

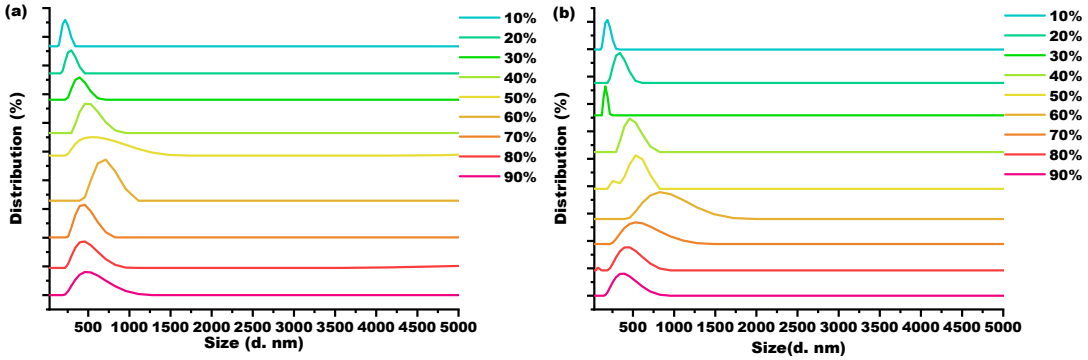

Figure S6. The DLS study on nanoparticle size distribution of (a) B-PDI-ANT and (b) O-PDI-ANT in THF/water mixture with different water fractions (f_w)

2.4 Femtosecond transient absorption spectra and kinetics fitting of B-PDI-ANT and O-PDI-ANT in THF

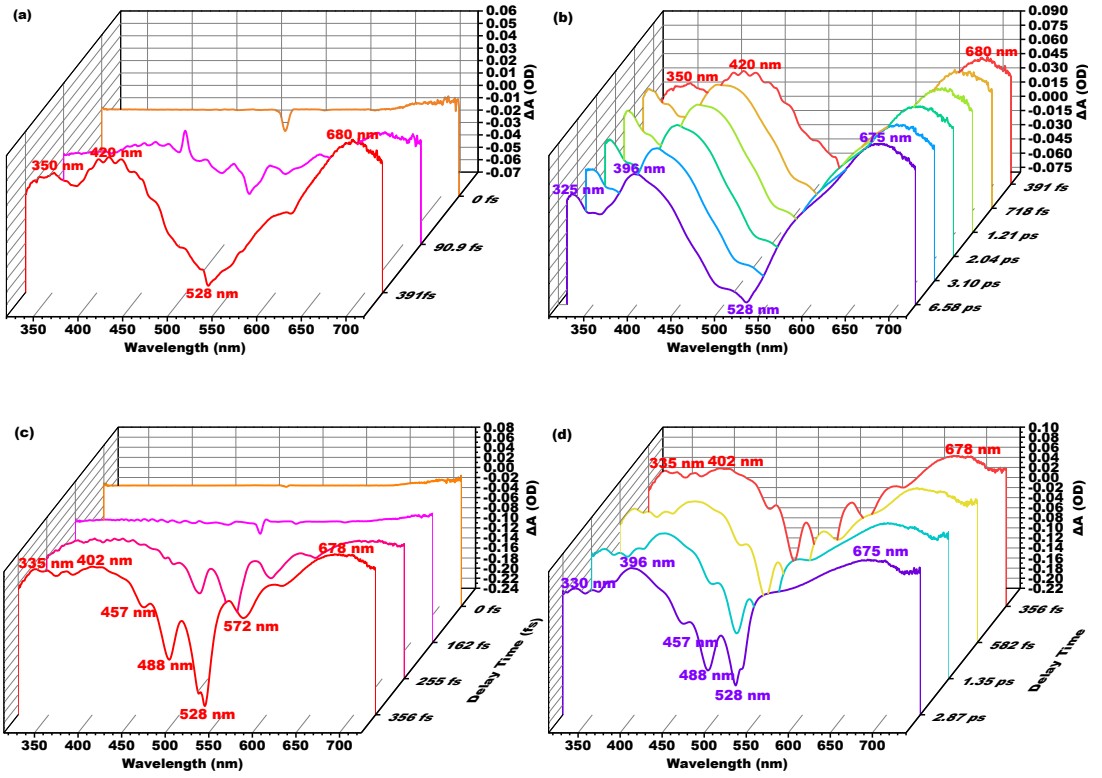

Figure S7. Femtosecond transient absorption spectra of (a, b) B-PDI-ANT and (c, d) O-PDI-ANT in THF.

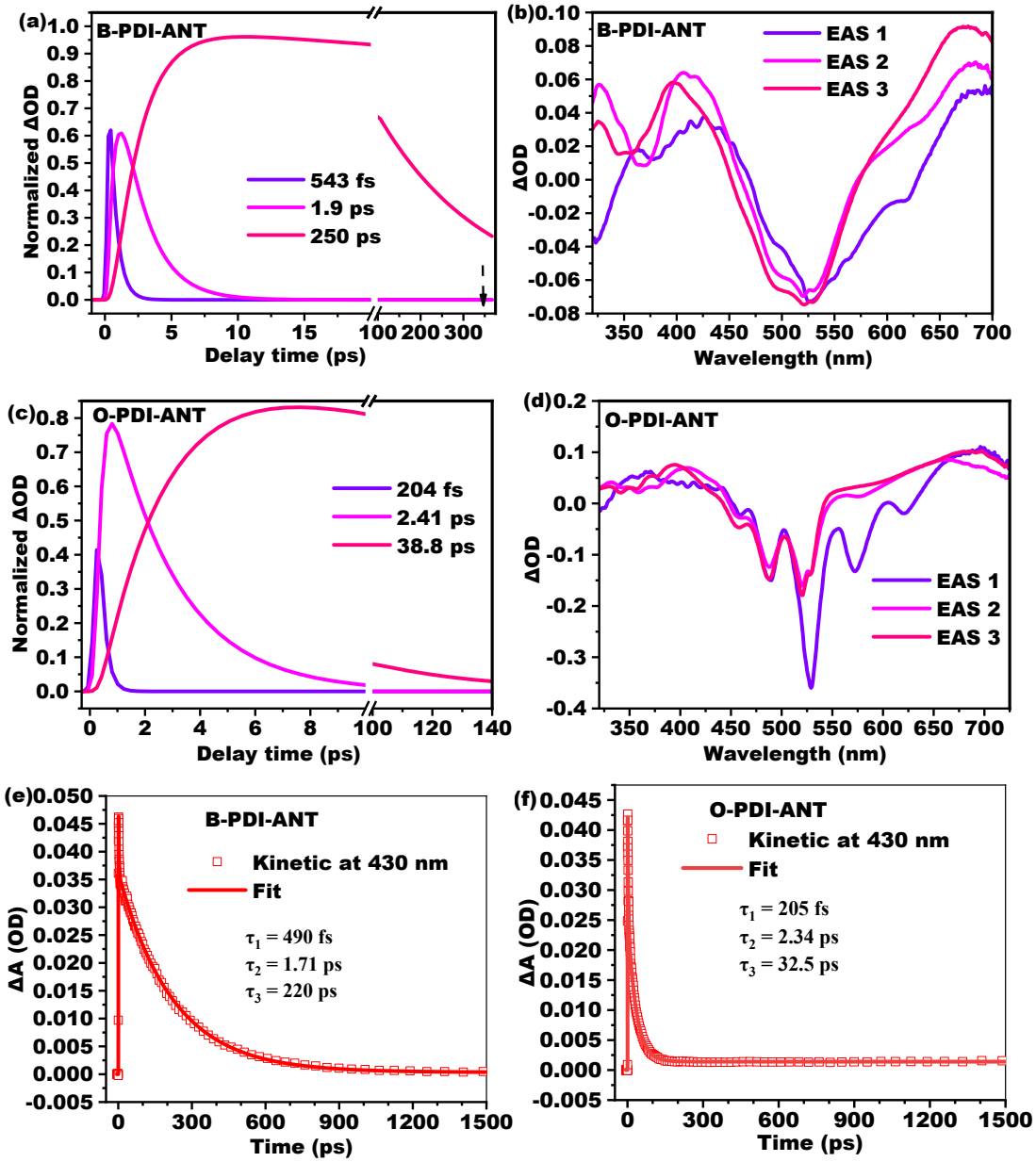

Figure S8. Global fitting (a-d) and wavelength fitting (e-f) of B-PDI-ANT and O-PDI-ANT in THF.

Table S1. Summary of the global fitting andwavelength fitting for B-PDI-ANT and O-PDI-ANT in THF

Sample	Fitting method	τ_1 (ps)	τ_2 (ps)	τ_3 (ps)
B-PDI-ANT	Global fitting	0.54	1.9	250
	Wavelength fitting at 430 nm	0.49	1.71	220
O-PDI-ANT	Global fitting	0.20	2.41	39
	Wavelength fitting at 430 nm	0.21	2.34	33

Global fitting of B-PDI-ANT at all wavelengths gives three time constants: 0.54 ps (τ_1), 1.9 ps (τ_2)

and 250 ps (τ_3). Wavelength fitting of B-PDI-ANT at 430 nm gives three very similar time constants: 0.49 ps (τ_1), 1.71 ps (τ_2) and 220 ps (τ_3). Global fitting of O-PDI-ANT at all wavelengths gives three time constants: 0.20 ps (τ_1), 2.41 ps (τ_2) and 39 ps (τ_3). Wavelength fitting of O-PDI-ANT at 430 nm also gives three very similar time constants: 0.21 ps (τ_1), 2.34 ps (τ_2) and 33 ps (τ_3).

2.5 Nanosecond transient absorption spectra and kinetics fitting of O-PDI-ANT in THF

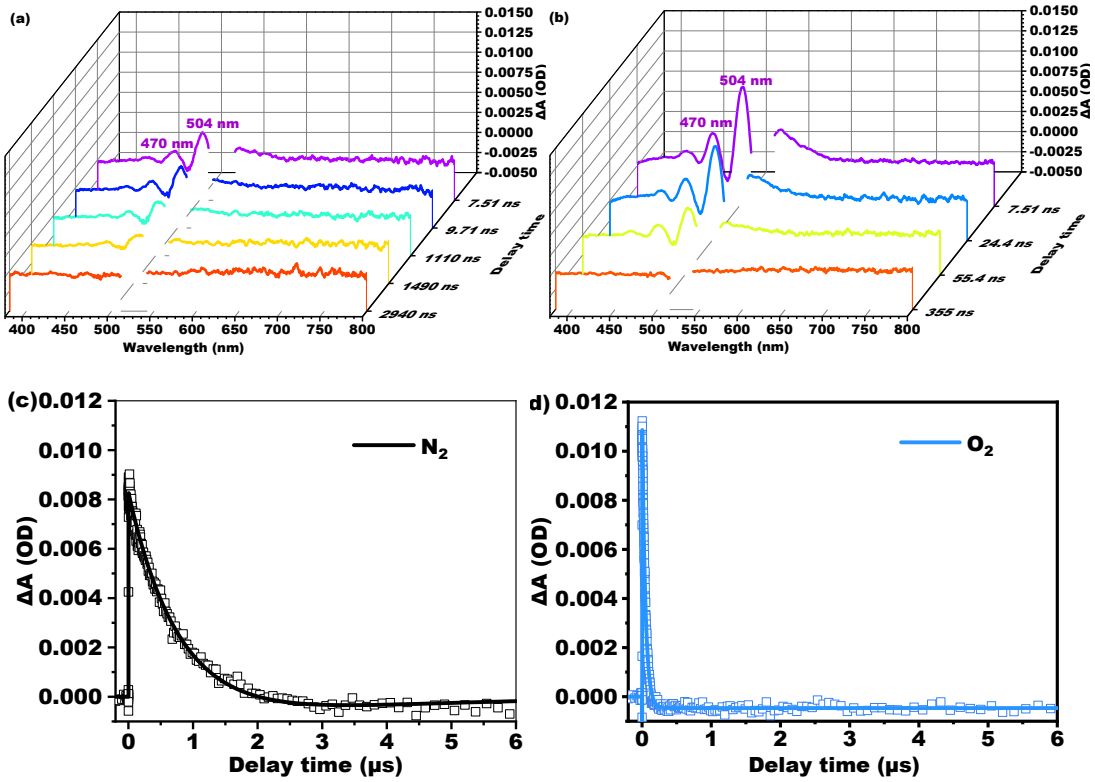

Figure S9. Nanosecond transient absorption spectra and kinetics fitting at 504 nm of O-PDI-ANT in THF purged with N_2 or O_2.

Figure S9a shows that the signals (470 and 504 nm) generated by ISC are gradually decreased to the baseline from 7.51 ns to 2.94 μs. The kinetic fitting at 504 nm shows that O-PDI-ANT has a long lifetime of τ_1 = 2.7 μs. When the solution is purged with oxygen (Figure S9b), the long-lifetime transient state is significantly quenched by the oxygen and the lifetime drops down to 0.0465 μs. This demonstrates that the long-lifetime transient state with main peaks at 470 and 504 nm of O-PDI-ANT has a triplet-state nature.

2.6 Femtosecond transient absorption spectra and kinetics fitting of B-PDI-ANT and O-PDI-ANT in THF-H_2O with different f_w

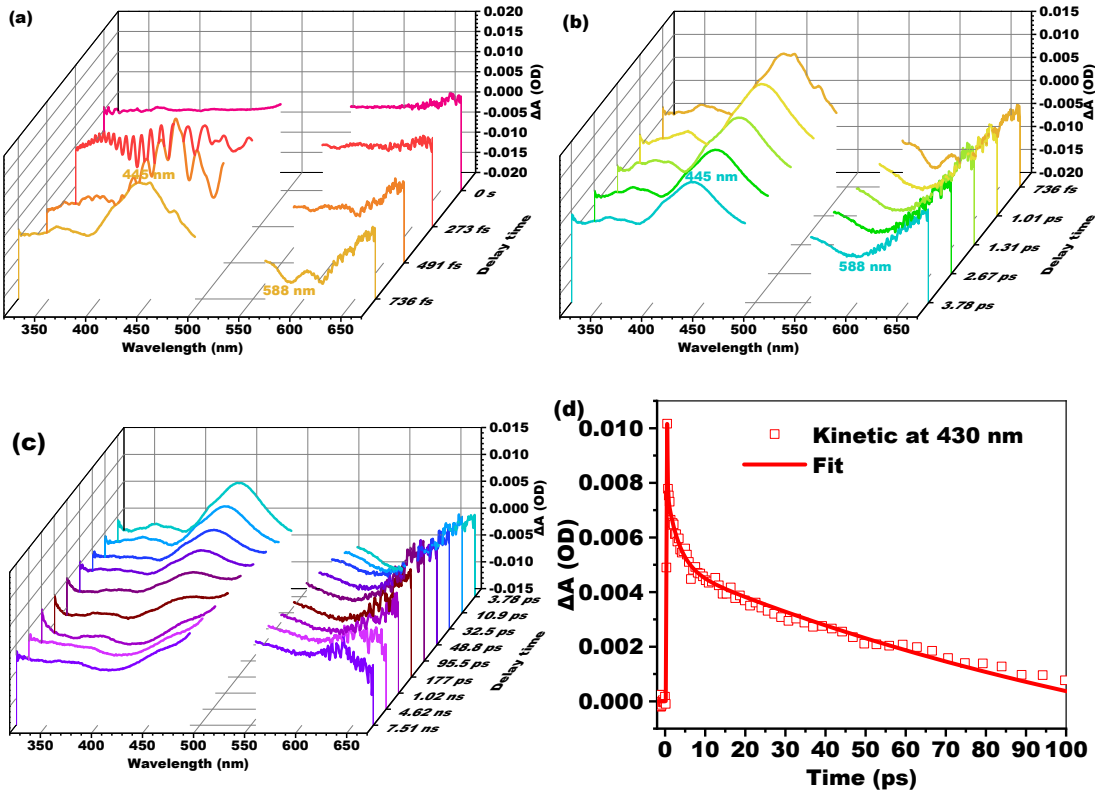

Figure S10. Femtosecond transient absorption spectra and kinetics fitting at 430 nm of B-PDI-ANT in THF/H_2O (f_w = 60%).

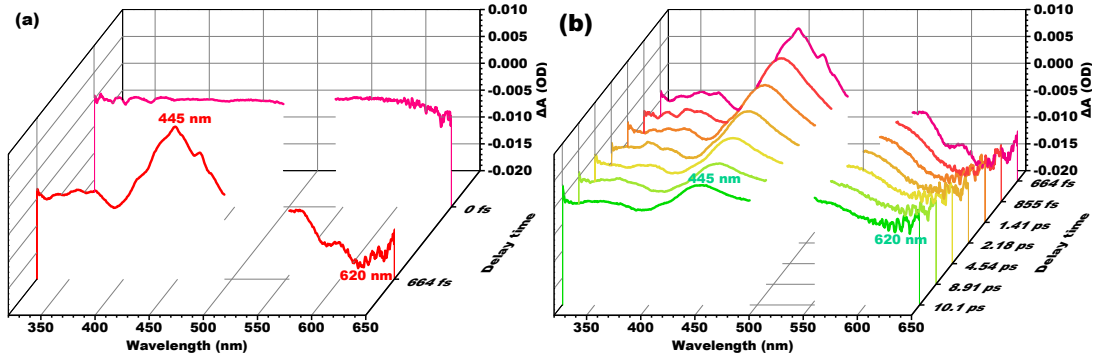

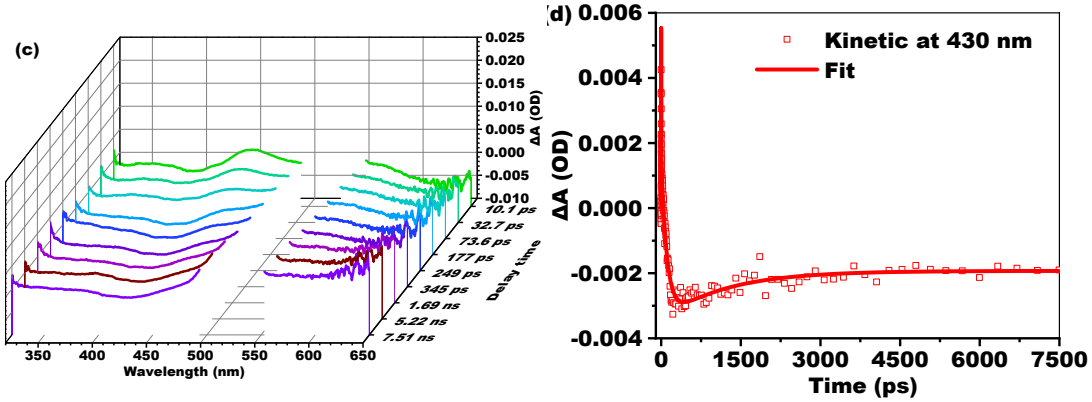

Figure S11. Femtosecond transient absorption spectra and kinetics fitting at 430 nm of B-PDI-ANT in THF/H_2O (f_w = 90%).

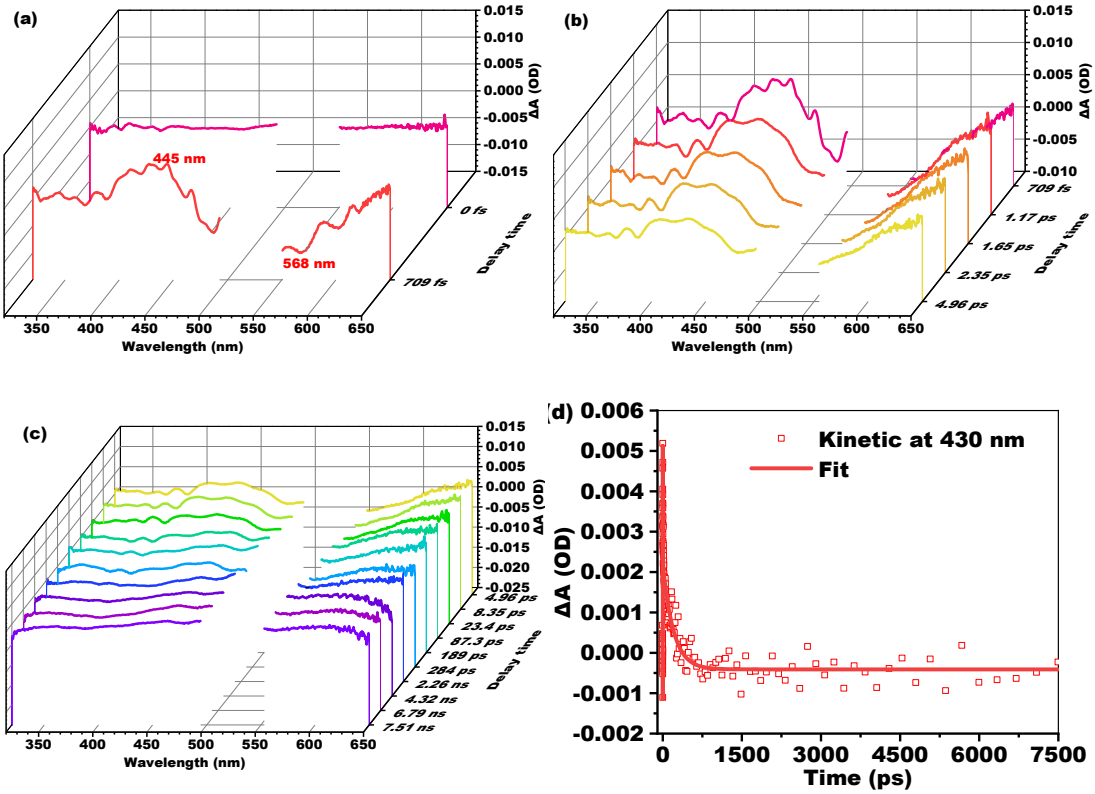

Figure S12. Femtosecond transient absorption spectra and kinetics fitting at 430 nm of O-PDI-ANT in THF/H_2O (f_w = 60%).

Table S2. Summary of the wavelength fitting for B-PDI-ANT and O-PDI-ANT at 430 nm in THF/H_2O with different f_w.

	f_w (%)	τ_1 (ps) (amplitude)	τ_2 (ps) (amplitude)	τ_3 (ps) (amplitude)
B-PDI-ANT	0	0.49 (33.5%)	1.71 (27.6%)	220 (38.5%)
	60	0.107 (44.6%)	2.99 (9.08%)	152 (31.3%)
	90	0.219 (71%)	3.73 (8.39%)	91 (14.9%)
O-PDI-ANT	0	0.205 (39.3%)	2.34 (28.6%)	32.5 (30.4%)
	60	0.0908 (80%)	2.75 (10.8%)	201 (7.95%)

2.7 The optimized XYZ coordinates

S_0 of B-PDI-ANT

C	-0.58618808	5.03748318	-0.05873647
N	-1.76167621	5.78252369	-0.11722340
C	-3.04979422	5.24308438	-0.12394493
C	-3.93362145	-4.77276934	0.10383292
N	-2.80517483	-5.51955123	-0.24042836
C	-1.55382627	-4.98354123	-0.53995257
O	-4.03446283	5.95684965	-0.16987688
O	0.49472067	5.59672252	-0.04423891
O	-4.99708425	-5.31025210	0.35241800
O	-0.63106426	-5.71612459	-0.84550608
C	-3.15287692	3.76562678	-0.07354246
C	-0.72504055	3.56399660	-0.01839038
C	-1.99710946	2.95753062	-0.04003187
C	-4.39627494	3.18067845	-0.05900177
C	-4.51318118	1.79001110	0.01342341
C	-3.40171054	0.96348801	0.05395243
C	-2.09949025	1.54447836	-0.01506729
C	-0.91163065	0.74202629	-0.03022416
C	0.32951814	1.37530379	0.11884893
C	0.39468033	2.78523534	0.09491955
C	-3.76847464	-3.30074646	0.14710415
C	-1.41474728	-3.51236166	-0.46365535
C	-2.51708662	-2.70288010	-0.11471943
C	-2.37159310	-1.29393841	-0.04873812
C	-3.52863731	-0.49538763	0.17104822
C	-4.73590987	-1.11938845	0.44135905
C	-4.85520107	-2.51264172	0.44441024
C	-0.21044684	-2.92613354	-0.76436298
C	-0.04687203	-1.53953411	-0.65071666
C	-1.08009879	-0.71194100	-0.23805167
H	-5.27404254	3.81572986	-0.09409893
H	-5.50739052	1.36146894	0.02814441
H	1.35703266	3.27594659	0.18586651
H	-5.61890071	-0.53001721	0.65495244
H	-5.80426743	-2.99169616	0.65629771
H	0.61554259	-3.55665053	-1.07362950
H	0.91809170	-1.12004066	-0.89177870
C	1.62157145	0.68463368	0.38924812
C	2.72916515	0.93611806	-0.36975371
C	1.73696720	-0.18444921	1.52563763

C	3.99254983	0.33602809	-0.07658520
H	2.66136852	1.59739850	-1.22956555
C	2.92222997	-0.76534401	1.84245175
H	0.85872763	-0.36250969	2.13738628
C	5.12316465	0.57497274	-0.85545090
C	4.09415553	-0.53744641	1.05458469
H	3.00029000	-1.41301554	2.71100837
C	6.35205822	-0.01654652	-0.55974000
H	5.04693654	1.23842432	-1.71330308
C	5.31962102	-1.12788628	1.35161492
C	7.51865370	0.21970738	-1.34960334
C	6.45315817	-0.89049332	0.57220077
H	5.39603052	-1.78957214	2.21080964
C	8.70458326	-0.37114679	-1.03788316
H	7.43792369	0.88305830	-2.20607055
C	7.71596522	-1.49028565	0.86438367
C	8.80483446	-1.23995410	0.08676276
H	9.58419099	-0.18370431	-1.64559837
H	7.78810843	-2.15207835	1.72282526
H	9.75925653	-1.70179111	0.31903502
C	-2.91888540	-6.97373168	-0.30863999
H	-3.93926008	-7.23843503	-0.04512766
H	-2.68164019	-7.31671797	-1.31722248
H	-2.21164254	-7.43248317	0.38439806
C	-1.60681648	7.23383146	-0.16370402
H	-1.08136971	7.57896477	0.72847566
H	-1.01777406	7.51433376	-1.03847189
H	-2.60030351	7.67089609	-0.21486010

S_1 of B-PDI-ANT

C	4.87348849	-2.59543153	0.27296758
N	6.08133590	-2.01695715	-0.11145880
C	6.24716942	-0.68358998	-0.50176374
C	-1.88330897	5.19222568	-0.20554478
N	-2.99267357	4.69159451	0.48403963
C	-3.06406200	3.43577259	1.08484315
O	7.34005236	-0.25568176	-0.83504395
O	4.82858783	-3.77733964	0.58056766
O	-1.90111469	6.30554444	-0.70514981
O	-4.08102412	3.09249219	1.66893345
C	5.04118064	0.16319766	-0.48644455
C	3.69292659	-1.71964962	0.28555615

C	3.80450973	-0.35641488	-0.09264706
C	5.14392509	1.50222067	-0.86638921
C	4.03224997	2.31796276	-0.86134435
C	2.76848009	1.83712227	-0.46710977
C	2.65117935	0.47877671	-0.06056223
C	1.40965368	-0.05947453	0.38747191
C	1.29470719	-1.48471375	0.57102091
C	2.46146834	-2.25967620	0.58153314
C	-0.70770877	4.30816284	-0.29181867
C	-1.87851945	2.57376281	0.96902439
C	-0.72827042	3.02660805	0.27609565
C	0.41146400	2.17946956	0.16128755
C	1.58605017	2.67195524	-0.46428967
C	1.56148249	3.96414672	-1.02470858
C	0.43635765	4.75997335	-0.94844234
C	-1.86966445	1.33893703	1.59675308
C	-0.77608875	0.49441917	1.47739166
C	0.34628607	0.85335841	0.68189032
H	6.11740060	1.87850986	-1.15910348
H	4.14761604	3.35656972	-1.14479316
H	2.41703533	-3.33097080	0.74098879
H	2.43474666	4.34491334	-1.53961567
H	0.41807864	5.75136563	-1.38631451
H	-2.73002839	1.05993759	2.19492713
H	-0.74255903	-0.40674785	2.07278006
C	0.01287575	-2.17676168	0.57673220
C	-1.06154089	-1.71491694	-0.19384831
C	-0.17074526	-3.38194689	1.32506745
C	-2.29813796	-2.39952851	-0.24027958
H	-0.92637140	-0.85283687	-0.83471703
C	-1.35510327	-4.05122169	1.31411087
H	0.64332744	-3.74259857	1.94302497
C	-3.36043742	-1.93901255	-1.02102358
C	-2.46665845	-3.59507414	0.53670192
H	-1.47694075	-4.94966878	1.91196918
C	-4.58718766	-2.61112800	-1.05676161
H	-3.23448734	-1.03224076	-1.60636049
C	-3.67845691	-4.26314603	0.50352925
C	-5.67829996	-2.14614709	-1.84334324
C	-4.75326407	-3.80037557	-0.27714609
H	-3.80636205	-5.16824596	1.09146544
C	-6.86529400	-2.82236042	-1.85723760
H	-5.54903085	-1.24173255	-2.43019811
C	-6.00016096	-4.47613869	-0.31787454

C	-7.02766993	-4.00072439	-1.08621546
H	-7.69216230	-2.45936239	-2.45865324
H	-6.12475971	-5.37834446	0.27358117
H	-7.97706455	-4.52578148	-1.10819650
C	-4.17901599	5.53226656	0.60444893
H	-5.03689274	5.03076987	0.15246245
H	-4.40360913	5.70737719	1.65818483
H	-3.97200987	6.46994140	0.09574262
C	7.24623198	-2.89548601	-0.11132352
H	7.39615441	-3.30998160	0.88712382
H	7.08696577	-3.72411255	-0.80402288
H	8.10575935	-2.30385731	-0.41464570

S_0 of O-PDI-ANT

C	5.28668909	-3.60927025	0.20370730
N	6.60883423	-3.17429657	0.11238055
C	6.96448659	-1.83524951	-0.10470007
C	-0.33777627	5.10681150	-0.26862708
N	-1.65408800	4.69582454	-0.10635240
C	-2.03946426	3.34563681	-0.04241978
O	8.12826695	-1.50896459	-0.25626294
O	5.00590027	-4.78974448	0.30551005
O	-0.04093906	6.27793964	-0.42901563
O	-3.21913321	3.05205551	-0.07509524
C	5.87850380	-0.82809811	-0.13493920
C	4.22030474	-2.57588921	0.17996541
C	4.53093227	-1.21166421	0.01274407
C	6.19463037	0.49811078	-0.30716428
C	5.18555915	1.46693538	-0.32991290
C	3.84857229	1.13401823	-0.18542732
C	3.50057046	-0.23777631	-0.01243955
C	2.14685157	-0.65946487	0.13382097
C	1.88434555	-2.01023722	0.29189780
C	2.90863569	-2.96330982	0.31415275
C	0.70589323	4.05518342	-0.23925247
C	-0.97693885	2.31020137	0.07002344
C	0.38144141	2.69114005	-0.07289480
C	1.42364093	1.72734172	-0.05478780
C	2.77851631	2.14618860	-0.20471329
C	3.04383647	3.49512951	-0.36401266
C	2.01734108	4.44162157	-0.38213633
C	-1.29769236	0.96940764	0.24839540
C	-0.25073340	0.02519469	0.25869419

C	1.08003195	0.35589424	0.11076388
H	7.23613248	0.77567156	-0.42207661
H	5.48065644	2.49949954	-0.46570669
H	0.86610413	-2.36056086	0.40292552
H	2.68615435	-4.01710076	0.43639481
H	4.06119553	3.84640085	-0.47891267
H	2.23238957	5.49637554	-0.50822067
H	-0.54126735	-1.00592029	0.41063856
C	-2.66646312	0.42226048	0.46704713
C	-3.41690160	0.78314341	1.63330489
C	-3.16917698	-0.51389923	-0.38760977
C	-4.61932074	0.21141224	1.89081328
H	-3.00468331	1.52083593	2.31324720
C	-4.44439633	-1.12068410	-0.16758531
H	-2.60862668	-0.80165539	-1.27316608
C	-5.18699030	-0.75487760	1.00121381
H	-5.17762617	0.48554878	2.78139961
C	-4.97946555	-2.05816414	-1.04823829
C	-6.42616420	-1.34583427	1.23229177
C	-6.22303925	-2.64967699	-0.81999943
H	-4.41683454	-2.33439867	-1.93672893
C	-6.96538820	-2.28440032	0.35034353
H	-6.98965696	-1.06775163	2.11957106
C	-6.78447393	-3.61049643	-1.71549955
C	-8.23684079	-2.89564300	0.57304664
C	-8.00001016	-4.17103237	-1.46767458
H	-6.21864491	-3.88401488	-2.60175765
C	-8.73795979	-3.80767236	-0.30456615
H	-8.79672984	-2.61527282	1.46091701
H	-8.41580213	-4.90004532	-2.15626467
H	-9.70593409	-4.26445589	-0.12402859
C	7.68256741	-4.16873838	0.25052100
H	7.93212338	-4.56041958	-0.71343326
H	8.54518634	-3.70474057	0.68121203
H	7.35195303	-4.96490015	0.88433546
C	-2.75712321	5.66748236	-0.09662167
H	-3.33678787	5.55797431	-0.98931256
H	-3.37911543	5.49244259	0.75624815
H	-2.35835556	6.65929112	-0.04971767

S_1 of O-PDI-ANT

C	-6.11359016	-3.05068784	0.01026919
N	-7.31062137	-2.36442661	0.24314240

C	-7.42443682	-0.98495234	0.41625096
C	0.97352563	4.48465626	-0.09820089
N	2.17713122	3.79626589	-0.31997519
C	2.28858173	2.42491840	-0.46424827
O	-8.52206362	-0.48580158	0.61539878
O	-6.10341175	-4.26533607	-0.13111588
O	0.96763746	5.70300809	0.01093668
O	3.42216842	1.94713136	-0.68528147
C	-6.18377562	-0.20042469	0.34607656
C	-4.89494502	-2.23442330	-0.05158020
C	-4.94586673	-0.83365478	0.11550602
C	-6.23549518	1.17276858	0.50928309
C	-5.07966455	1.93558441	0.44489389
C	-3.82699769	1.35376425	0.21563687
C	-3.75015827	-0.05959307	0.05156376
C	-2.50380767	-0.72003059	-0.17656850
C	-2.50714085	-2.11374039	-0.34213035
C	-3.67662297	-2.85250181	-0.28049240
C	-0.22777228	3.65899473	-0.01677840
C	1.09336167	1.62564269	-0.33694380
C	-0.16203906	2.25877728	-0.14055100
C	-1.36494717	1.48576618	-0.07191205
C	-2.60679447	2.14474713	0.13832625
C	-2.61563054	3.54421166	0.26351272
C	-1.45675096	4.28489593	0.18670173
C	1.13717929	0.21670684	-0.45601087
C	-0.03031120	-0.51788503	-0.41367523
C	-1.29386093	0.06883610	-0.22549316
H	-7.20088255	1.63331172	0.68739815
H	-5.16646296	3.00573897	0.57933312
H	-1.58127317	-2.64289828	-0.52743588
H	-3.66528919	-3.92904689	-0.40947194
H	-3.54994029	4.06772678	0.41829859
H	-1.47097082	5.36455458	0.28008701
H	0.04832753	-1.59481632	-0.49097846
C	2.41917149	-0.50662857	-0.59469186
C	2.61246552	-1.43706178	-1.63076444
C	3.46482535	-0.28776258	0.31684638
C	3.80576674	-2.10695106	-1.77915392
H	1.80786464	-1.60108347	-2.33797488
C	4.69928543	-0.95835983	0.19425608
H	3.30267151	0.36240380	1.16586755
C	4.88727077	-1.88876632	-0.88403763
H	3.93723425	-2.80993476	-2.59593619

C	5.73853933	-0.74328845	1.09762914
C	6.10020509	-2.54930708	-1.00972788
C	6.96966586	-1.41008965	0.97524519
H	5.59744570	-0.03623721	1.90986726
C	7.15693867	-2.33184752	-0.10184487
H	6.24360144	-3.25381182	-1.82435032
C	8.03193489	-1.19246970	1.88679342
C	8.39720314	-2.99994366	-0.22368220
C	9.22343668	-1.85647588	1.74009271
H	7.88751554	-0.49087213	2.70242919
C	9.40711691	-2.76695330	0.67710989
H	8.53909344	-3.69983247	-1.04135840
H	10.03160464	-1.68348138	2.44245586
H	10.35488834	-3.28435456	0.57398353
C	3.40488540	4.57321536	-0.44409201
H	4.12201469	4.26356623	0.31873166
H	3.85525622	4.40629145	-1.42437581
H	3.13963076	5.61939401	-0.31697488
C	-8.55104983	-3.12631778	0.31488769
H	-9.02188508	-2.97915754	1.28885010
H	-9.24550724	-2.77911324	-0.45266015
H	-8.30336006	-4.17344955	0.16272989

2.8 The optimized molecular orbital (MO) diagrams of B-PDI-ANT and O-PDI-ANT

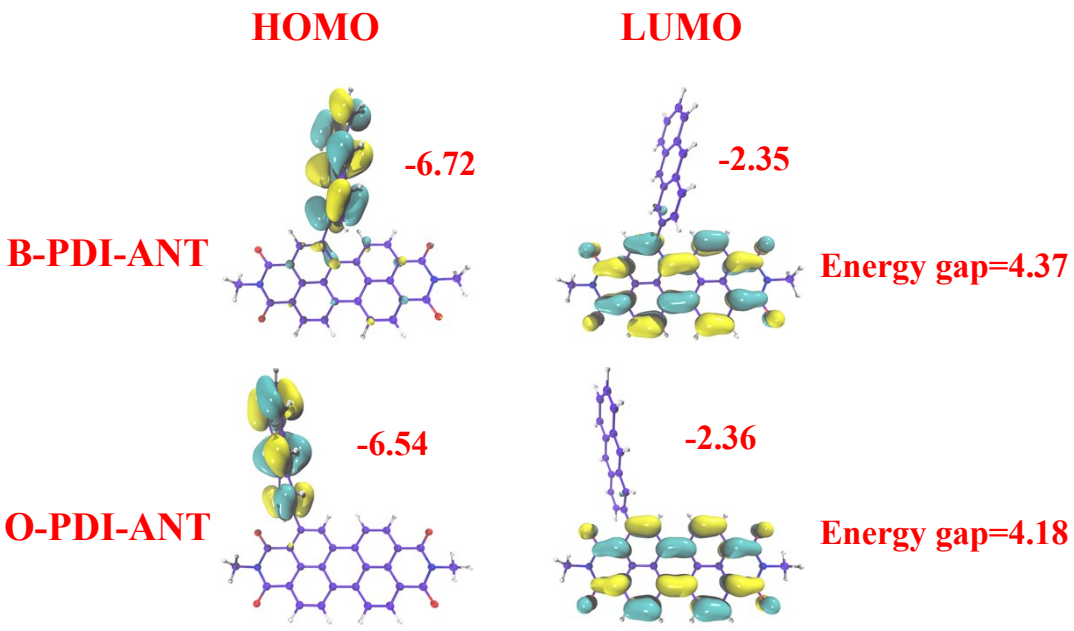

Figure S13. The optimized HOMO, LUMO and energy gap of B-PDI-ANT and O-PDI-ANT.

As shown in Figure S13, B-PDI-ANT and O-PDI-ANT exhibit the charge-transfer nature for the spatially separated HOMOs and LUMOs. Their HOMOs are restricted on the ANT groups, while LUMOs are distributed to the PDI core.

2.9 The open-aperture z-scan curves of B-PDI-ANT and O-PDI-ANT

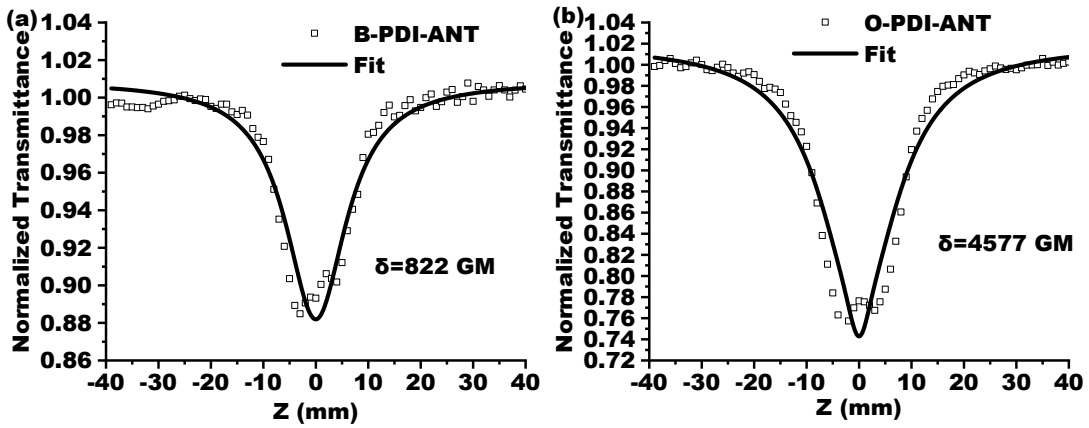

Figure S14. Open-aperture z-scan measurement of B-PDI-ANT and O-PDI-ANT at 1100 nm in THF solution.

2.10 The summary of the previously reported 2PA data for small organic molecules containing one or two PDI unit in recent ten years from 2011-2021

Table S3. Summary of the previously reported 2PA data for small organic molecules containing one or two PDI unit in recent ten years from 2011-2021.

Dyes	Method	Solvent	λ_{2PA}/ nm	δ/ GM	AIE/ACQ or unreported	Reference
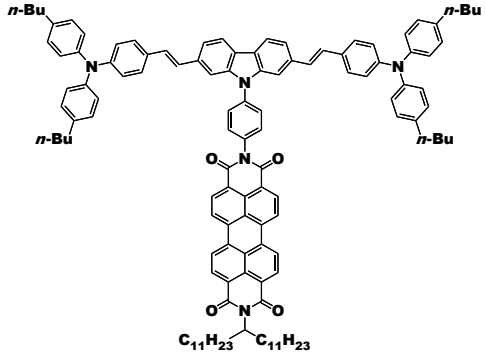	fs-TPEF	toluene	625	1075	unreported	31a

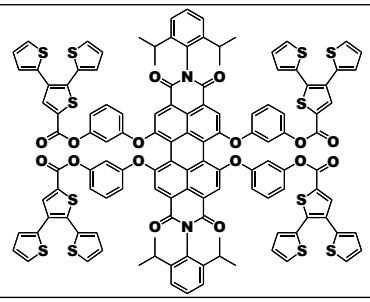	fs-TPEF	dichloro methane	720	324	unreported	31b
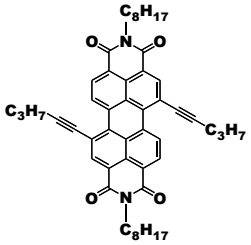	fs-TPEF	toluene	669	470	unreported	31c
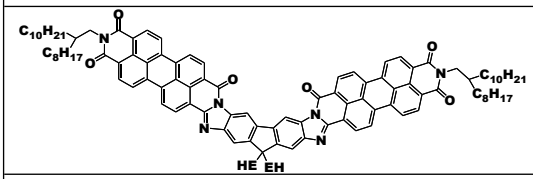	fs-TPEF	toluene	1220	1110	unreported	31d
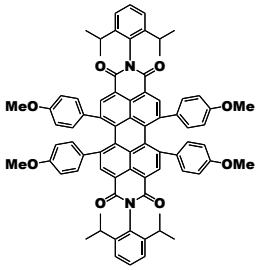	fs-TPEF	acetonit rile	850	180	unreported	31e
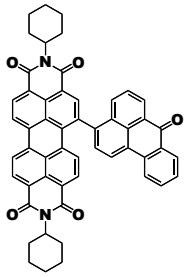	fs Z-scan	dichloro methane	800	1073	unreported	31f
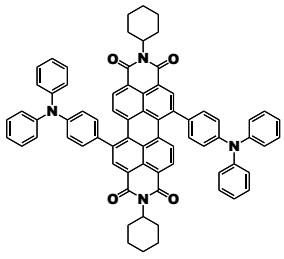	fs Z-scan	dichloro methane	900	140	unreported	31g

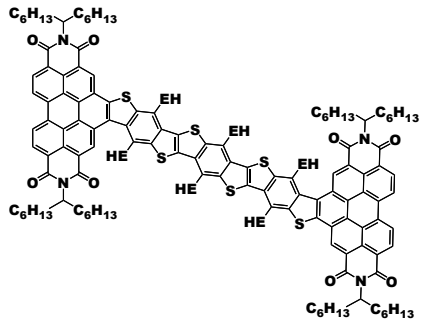	fs-TPEF	chloroform	800	125	unreported	31h
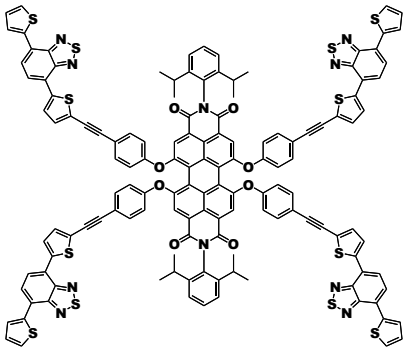	fs Z-scan	dichloromethane	639	3340	unreported	31i
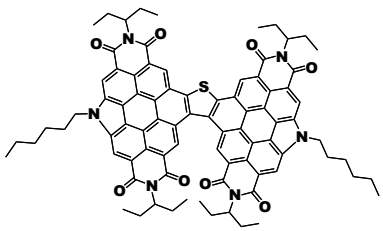	fs-TPEF	chloroform	800	18.4	unreported	31j
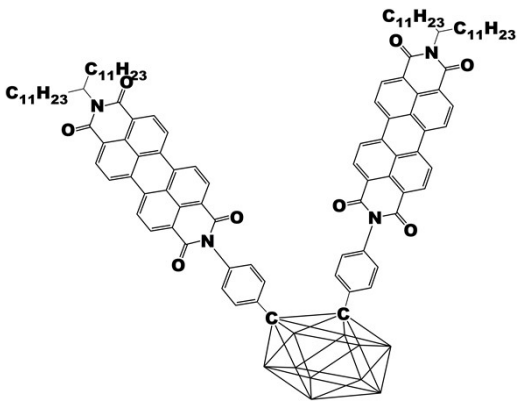	fs Z-scan	THF	650	2400	unreported	31k

3. Application

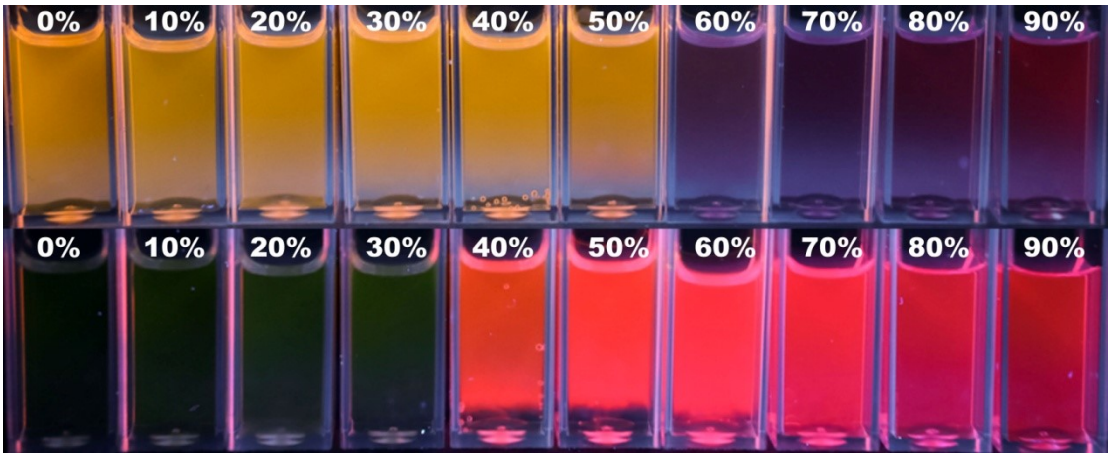

Figure S15. The photographs of fluorescence images (taken under 365 nm UV light) of (above) B-PDI-ANT and (below) O-PDI-ANT in THF/water mixture with different water fractions (f_w).

4. References

1. Holman, M. W.; Liu, R.; Adams, D. M., Single-Molecule Spectroscopy of Interfacial Electron Transfer. *Journal of the American Chemical Society* **2003**, *125* (41), 12649-12654.

2. Davis, N. J. L. K.; MacQueen, R. W.; Roberts, D. A.; Danos, A.; Dehn, S.; Perrier, S.; Schmidt, T. W., Energy transfer in pendant perylene diimide copolymers. *Journal of Materials Chemistry C* **2016**, *4* (35), 8270-8275.

3. Xu, L.; Li, Y.; Jiang, R.; Qin, Z.; Li, Y., 2,6-Anthracenyl(anthraquinonyl)-substituted difluoroboron dipyrromethenes: Synthesis, spectroscopy, electrochemistry and quantum chemical calculations. *Dyes and Pigments* **2014**, *107*, 90-96.

4. Teraoka, T.; Hiroto, S.; Shinokubo, H., Iridium-Catalyzed Direct Tetraborylation of Perylene Bisimides. *Organic Letters* 2011, *13* (10), 2532-2535.

5. Han, H.; Ma, L.-K.; Zhang, L.; Guo, Y.; Li, Y.; Yu, H.; Ma, W.; Yan, H.; Zhao, D., Tweaking the Molecular Geometry of a Tetraperylenediimide Acceptor. *ACS Applied Materials & Interfaces* **2019**, *11* (7), 6970-6977.